J Inorg Organomet Polym (2016) 26:1066–1074
DOI 10.1007/s10904-016-0426-3

Size Control in Porosity of Hydroxyapatite Using a Mold of Polyurethane Foam

C. S. Sipaut[1] · M. Jafarzadeh[2] · M. Sundang[1] · N. Ahmad[3]

Received: 18 May 2016 / Accepted: 22 July 2016 / Published online: 26 July 2016

Abstract The optimum sized polyurethane foam (PUF) was used as a mold for the formation of porous hydroxyapatite, HAp (calcium phosphate cement-base). Four PUFs of different formulations were selected based on their cell size and the percentage of open cell structure. In the preparation of porous HAp, tetracalcium phosphate and dicalcium phosphate anhydrous were mixed at a molar ratio of 1:1 in the presence of a cement setting solution namely, sodium phosphate. The effects of the morphology and the cell size of PUF on the HAp morphology were analyzed with a scanning electron microscope. Based on the analysis, it was observed that only PUFs with an average cell size of approximately 600 μm and a 95 % open cell structure could optimally generate porous HAp. This result showed 35 % enhancement in porosity compared to the reported values. This porous HAp fulfiled the two criteria for an ideal porous implant which include a cell size of more than 100 μm and a high percentage of open cell content (>50 %).

Keywords Ceramics · Chemical synthesis · Electron microscopy · Microstructure · Mechanical properties

✉ C. S. Sipaut
css@ums.edu.my

[1] Chemical Engineering, Faculty of Engineering, Universiti Malaysia Sabah, UMS Road, 88400 Kota Kinabalu, Sabah, Malaysia

[2] Faculty of Chemistry, Razi University, Kermanshah 67149-67346, Iran

[3] School of Chemical Sciences, Universiti Sains Malaysia, 11800 Penang, Malaysia

1 Introduction

Advances in the formulation of artificial materials as reliable substitutes have resulted in the increased usage of materials such as ceramic including hydroxyapatite (HAp), tricalcium phosphate (TCP), and calcium phosphate cement (CPC) in the fields of medicine and dentistry. As ceramics possess physical characteristics such as good bioactivity, biocompatibility, osteoconductivity and are able to promote bone growth [1], they have been extensively utilized as substitute implant materials in arthrodesis, reconstructive or cosmetic surgery, maxillofacial surgery, arthroplasty, orthodontics and other surgical and non-surgical therapies. However, ceramics have several drawbacks for use as bone grafting material due to their reactivity to the pharmaceuticals used in chemotherapy as well as their deleterious effects in respiratory processes, haemorrhaging, and infection [1, 2].

Hydroxyapatite (HAp) is a common artificial material used in bone implants and bone cement applications due to its similarities between the chemical composition of HAp [$Ca_{10}(PO_4)_6OH_2$)] and the chemical compositions of human bone and teeth. Synthetic HAp is normally used as the material for bone regeneration in diverse medical fields such as in orthopaedic surgery, dentistry, maxillofacial surgery and reconstructive surgery. In order to obtain its optimal field properties, parameters such as density, pore shape, pore size and pore interconnection pathway should be controlled. Porosity is a necessary attribute for in vivo bone tissue in-growths since good porosity facilitates the loading of proper cells into the porous materials and implanting the cell-loaded scaffold into the host body to promote bone tissue regeneration [3, 4]. Several studies have investigated the minimum pore size required to regenerate mineralized bone.

Mastrogiacomo et al. [3] reported that density and pore interconnectivity play significant roles in the bone regeneration process, as HAp with smaller pores and smaller interconnection sizes facilitated the faster formation of bone tissue.

Currently, materials with highly controlled porous structures are produced via the slurry crystal mold procedure using monodispersed polymers such as polyethylene, polyactide, poly(vinyl alcohol) and polystyrene. This procedure consists of three stages: the first stage was the formation of slurry crystal (i.e. monodispersed spheres) as a mold. Next, a ceramic precursor was added to the slurry crystal. Subsequently, the mold was removed from the ceramic via either heat or chemical treatment. The advantages derived from the process include high porosity, high pore interconnectivity and controllable pore size [4, 5].

Madhavi et al. [5] produced macroporous HAp with a pore size of 0.8–0.9 μm using ordered polystyrene sphere molds that were infused with a calcium phosphate precursor solution. Following that the mixture was sintered at temperatures ranging from 500 to 1000 °C in flowing oxygen to facilitate polymer removal and phosphate crystallization. McQuire et al. [6] fabricated HAp sponges by using amino acid-coated HAp nanoparticles dispersed within a viscous polysaccharide (dextran sulfate) matrix. In this process, the nanoparticles were prepared in the presence of excess amounts of aspartic acid, alanine and arginine. These nanoparticles were then organized into macroporous frameworks through the thermal degradation of dextran gel under controlled heating. Miao et al. [7] formulated a novel process to prepare porous HAp-based calcium phosphate ceramics containing micropores of about 5 μm in size by coating polyurethane (PU) foams with calcium phosphate cement (CPC) which were then heated at 1200 °C to improve the thickness of its struts. The porous HAp-based ceramics obtained had high porosity values of approximately 70 % and contained macro- and micropores that were highly interconnected [8]. PUFs are used in many applications because they are easy to handle and possess excellent properties such as versatile (open or closed cell), chemically resistant and lightweight [9]. Furthermore, PUFs can be synthesized using different chemicals to produce varied flexible foam with an open cell structures, limited resistance to applied loads and permeable to air.

In this study, we report the preparation of porous HAp using the designed PU template via the mold process. The PU foams with pore sizes of between 300 and 1000 μm were prepared in our lab and the results were published elsewhere [10]. An aqueous solution of Na_2HPO_4 (SP) was used as the liquid component for HAp preparation.

2 Materials and Methods

2.1 Preparation of Polyurethane (PU) Foams

Polyurethane foams (PUF) with various morphologies were prepared using the two-shot method. The chemicals are listed here used for the preparation of PUF: poly(ethylene glycol)-*block*-poly(propylene glycol)-*block*-poly(ethylene glycol) (M_n = ~4400 g mol^{-1}) (polyol), diphenylmethane 4,4′-diisocyanate, toluene diisocyanate, polydimethylsiloxane (surfactant), stannous octoate (organometallic catalyst), *N,N*-dimethylcyclohexamine (amine catalyst), and distilled water (blowing agent). The amount of each component was based on 100 parts of weight of total polyol. All the ingredients, except isocyanate, were mixed into a 12-ounce paper cup and agitated for 30 s at 1100 rpm using a 10-inch shop drill equipped with a 3-inch diameter-mixing blade. At the end of the mixing period, a pre-measured quantity of isocyanate was added to the cup and further agitated for an additional 5 s. The resulting foam was allowed to rise and cure for 6 min. Subsequently, the foam was removed from the mold and cut into small pieces using a foam cutter. The physical characteristics and cell morphologies of PUFs derived from diverse formulations under different conditions are brought in following: PUF 25-300 (25 % open cell, ~300 μm cell size), PUF 60-600 (60 % open cell, ~600 μm cell size), PUF 95-600 (95 % open cell, ~600 μm cell size) and PUF 98-1000 (98 % open cell, ~1000 μm cell size). The details can be found in our published report [10].

2.2 Preparation of Porous HAp

The synthesis of porous HAp (based on calcium phosphate ceramics) involved three basic steps; the synthesis of tetracalcium phosphate (TTCP powder), the synthesis of flowable calcium phosphate cement (CPC slurry) and the production of porous HAp using PUF.

TTCP powder was synthesized via a solid-to-solid reaction between pyro-calcium phosphate (CPP, Aldrich) and calcium carbonate (CC, Nacalai tesque) at a temperature of 1320 °C [11]. The CPP powder was mixed with the CC powder in an ethanol solution with the weight ratio of CPP to CC at 1:1.27. After 2 h, the mixture was dried and crushed into fine powder. The mixture was calcined in an alumina crucible at 1350 °C for 5 h at a heating rate of 10 °C min^{-1} in atmospheric air to produce TTCP powder [7]. This was followed by direct quenching in open air at 25 °C. The quenched powder was then crushed into fine powder and stored in a desiccator.

The CPC powder was synthesized by mixing dry TTCP powder with dry dicalcium phosphate anhydrous (DCPA,

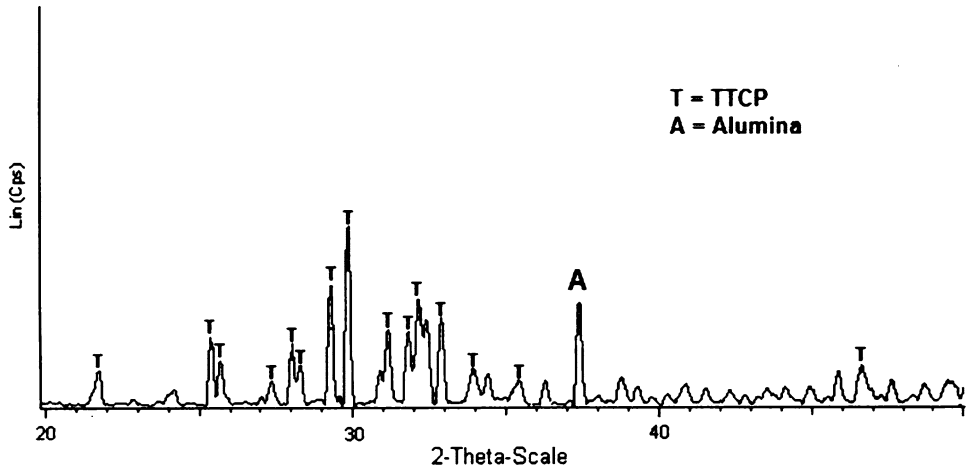

Fig. 1 The XRD pattern of the TTCP powder

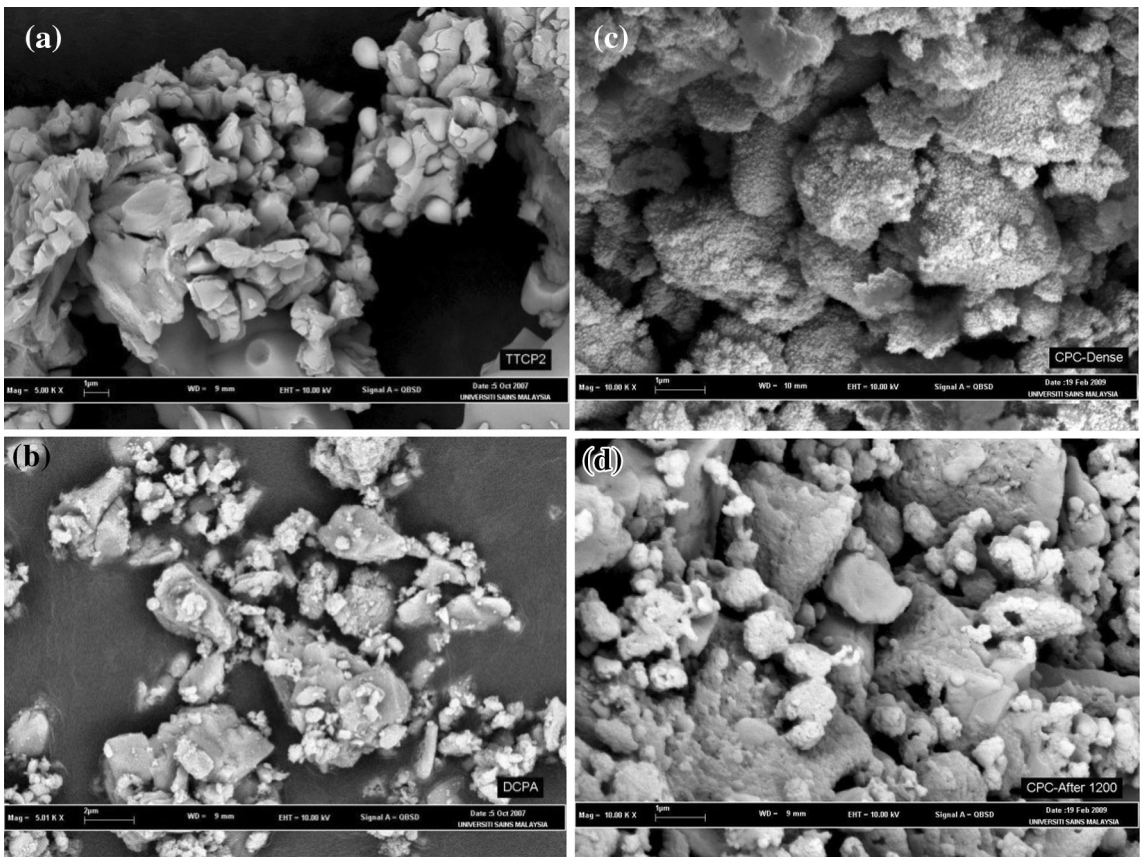

Fig. 2 SEM micrographs of **a** TTCP, **b** DCPA, and a fracture surface of the **c** set CPC and **d** fired CPC

Fluka) powder in a jar placed within a vibration mill. The molar ratio of TTCP to DCPA was 1:1, while the weight ratio was 72.9:27.1. An aqueous solution of Na_2HPO_4 (SP, Aldrich) was used as the liquid component for HAp preparation. In contrast, the use of distilled water without SP considerably decelerated the reaction time by more than 60 min. In order to produce porous HAp, the liquid component (SP) was added slowly into the CPC in varying volumes (i.e. 0.75–0.9 mL per every gram of CPC sample) to obtain varying viscosity slurry. Next, the CPC slurry was used to coat the PUF. Subsequently, the CPC-coated foams were allowed to set for more than 24 h. This sample will be known as set CPC.

To remove the residual PUF, the CPC-coated foam was fired in air in an electric furnace using a four-stage procedure. Firstly, the CPC-coated foam sample was heated

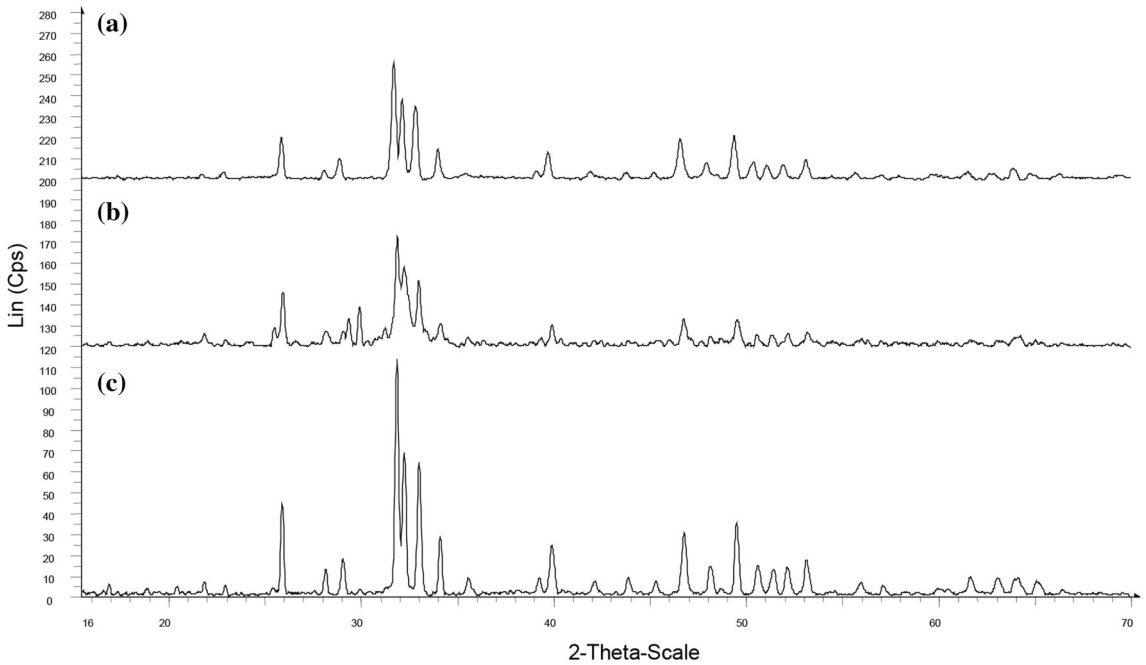

Fig. 3 XRD patterns of (*a*) pure HAp, (*b*) set CPC and (*c*) sintered CPC

from 40 to 600 °C at a heating rate of 1 °C min^{-1}. Secondly, the temperature was raised from 600 to 1200 °C at 5 °C min^{-1}. Then, the temperature was held at 1200 °C for 2 h, and finally the CPC foam was left to cool down to 40 °C at a cooling rate of 5 °C min^{-1}. This sample will be known as sintered CPC or CPC-based HAp.

2.3 Characterization Techniques

The crystal structure of samples was characterized using an X-ray diffractometer (XRD) (SIEMENS D5000, Cu Kα radiation). The morphology and elemental composition were examined using a field emission scanning electron microscope (FESEM, Leo Supra 50 VP) equipped with energy dispersive X-ray microanalysis system (EDX, Oxford INCA 400). The specimen was sputtered with a thin layer of gold (20 nm). The percentage (P) of open cells was calculated from scanning electron microscope (SEM) images according to the formula reported in our previous articles [10]. The pore sizes were obtained by applying SEM images and a formula from a reported article [12]. The content of aluminum in the immersed TTCP and porous HAp in a standard aluminum nitrate ($Al(NO_3)_3$-$9H_2O$) solution was determined by using an atomic absorption spectrophotometer (AAS), Perkin Elmer Precisely Analyst 200. The thermal analysis was performed using a Mettler Toledo (TGA/SDTA 851^e) model under a nitrogen flow with a heating rate of 10 °C min^{-1}. The mechanical properties (compressive strength) were determined using a Hounsfield Test Equipment Ltd set at a crosshead speed of 10 mm min^{-1}. Compressive strength was conducted on the six samples to determine the value of compressive stress and compressive strain at 50 %.

3 Results and Discussion

3.1 Preparation of Tetracalcium Phosphate (TTCP)

The following reaction is assumed for the synthesis of the TTCP powder. The TTCP was synthesized from a reaction between pyro-calcium phosphate and calcium carbonate.

$$Ca_2P_2O_7 + 2CaCO_3 \rightarrow \underset{\text{TTCP}}{Ca_4(PO_4)_2O} + 2CO_2 \quad (1)$$

XRD analysis was used to examine the phase transformation of TTCP. Figure 1 shows the XRD patterns of the sample powder after direct quenching in air. The data indicates that the XRD patterns of the samples were matched with the standard patterns (JCPDS no. 25-1137). This finding supports that of Guo et al. [11], who observed that initial cooling in dry air at a faster cooling rate contributed to the formation of pure TTCP during the subsequent cooling process. The existence of peak A, as seen in Fig. 1, was indicative of contamination caused by the utilization of aluminum from the crucible, a finding attested to by the presence of 0.973 ± 0.1345 ppm of aluminum ions when the sample was subjected to atomic absorption spectroscopy analysis. This finding was in accordance with other studies in which a platinum crucible was used in the

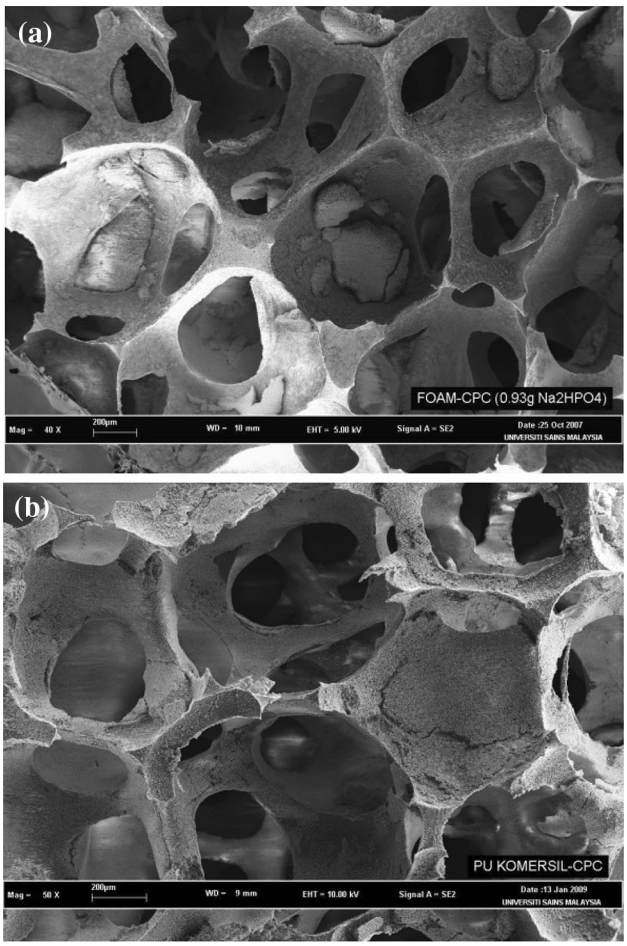

Fig. 4 SEM micrographs of PUFs were coated with: **a** low viscosity and **b** medium viscosity of CPC slurry

CPP and CC calcinations process to avoid contamination [9].

3.2 Preparation of Flowable Calcium Phosphate Cement (CPC Slurry)

TTCP and dicalcium phosphate anhydrous (DCPA) constitute the basic raw materials in the production of calcium phosphate cements (CPCs). Na_2HPO_4 (SP) solution is generally added to the mixture in order to accelerate the formation of hydroxyapatite crystals during the setting phase. During the setting, the following reaction is expected:

$$\underset{\text{TTCP}}{2Ca_4(PO)_2O} + \underset{\text{DCPA}}{2CaHPO_4} \rightarrow \underset{HA_p}{Ca_{10}(PO_4)_6(OH)_2} \quad (2)$$

Calcium and phosphate ions are precipitated by dissolving TTCP and DCPA, which in turn combine to form CPC. In fact, the real reaction is more complex than the above simple representation. Reaction 2 represented the non-existence of SP in the setting reaction. The SP was added into the water solution to catalyze the precipitation reaction between TTCP and DCPA. The addition of catalyst was reduced the reaction time by 60 min [7].

The morphology of both TTCP and DCPA powders are illustrated in Fig. 2a, b. It depicts that both powders are formless with specific surface areas of 0.88 $m^2\ g^{-1}$ and 1.18 $m^2\ g^{-1}$, respectively. Figure 2c shows the SEM micrograph of the fracture surface of set CPC. The hydroxyapatite crystals (whisker-like) were formed on the fracture surfaces of the set CPC [11]. Figure 2d also shows the fractured surface of sintered CPC. It clearly illustrated that sintered CPC had a smoother fracture surface than the set CPC. Moreover, there was a clear absence of whisker-like structures. This feature could plausibly be attributed to the increased density of hydroxyapatite crystals after being subjected to high temperatures [13]. This finding was supported by XRD analysis. Figure 3a, b shows the XRD patterns of the pure HAp and the set CPC. It was evident that the XRD peaks attributed to the set CPC were similar to the XRD peaks of pure hydroxyapatite. Figure 3c show the XRD pattern of sintered CPC. It can be clearly seen that the hydroxyapatite phase remained intact in the sintered CPC that was fired at 1200 °C for 2 h. It can be deduced that the hydroxyapatite phase formed at room temperature remained intact at up to temperatures of 1200 °C.

3.3 Preparation of Porous HAp Using PUF and CPC Slurry

PUFs in different cell sizes were coated with CPC slurry of varying viscosities. Figure 4 depict the results of the SEM analysis on the CPC-coated PUF samples. It is evident that CPC slurry of medium viscosity (0.75 mL SP = 1 g powder of CPC) could evenly penetrate and coat PUF cells when compared to CPC slurry of low viscosity (0.9 mL SP = 1 g powder of CPC). Based on this experiment, CPC slurry of medium viscosity was selected for use in the preparation of porous HAp.

PUFs with different cell sizes were used as molds for production of porous HAp via dipping the PUFs in the CPC slurry. The coated foam was squeezed and inflated with air at room temperature to remove loosely and non-homogenous attachment of the CPC slurry from the surface of CPC-coated scaffold. The CPC-coated foam was allowed to set and dry. Figure 5 shows the SEM micrographs of coated PUFs with different PUF molds. They show that all PUFs were well infiltrated by the CPC slurry.

Figure 6 shows the block of porous HAp, which was subjected to high temperatures. It is evident that the porous sintered CPC, Fig. 6a, remained structurally intact and was self-supporting when compared to the other samples. A

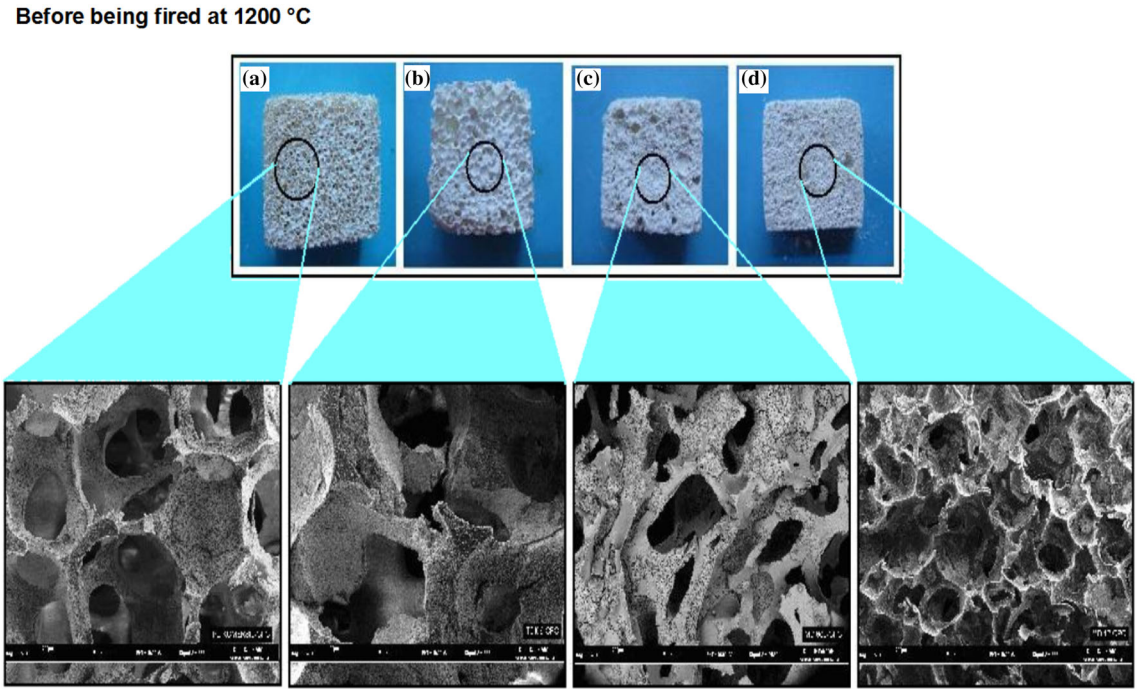

Fig. 5 SEM micrographs of CPC-coated PUFs using different molds: (*a*) PUF 95-600 (*b*) PUF 98-1000 (*c*) PUF 60-600 and (*d*) PUF 25-300. SEM scale bars were 200 μm

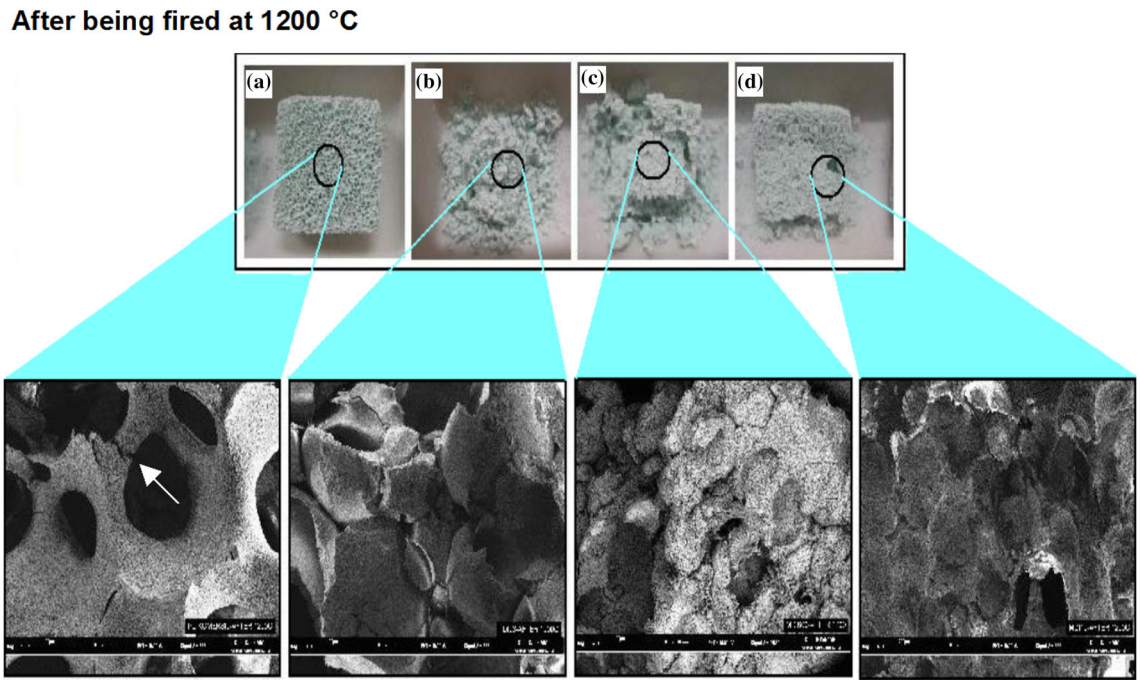

Fig. 6 SEM micrographs of sintered porous HAps using different molds: (*a*) PUF 95-600 (*b*) PUF 98-1000 (*c*) PUF 60-600 and (*d*) PUF 25-300. SEM scale bars were 200 μm

close analysis of the SEM micrograph indicates that sintered CPC had a porosity value exceeding approximately 50 %. Nevertheless, this relatively high porosity value was compromised by the presence of cracks in its struts (refer to Fig. 6a), which implies that it lacked sufficient strength to bear its own load.

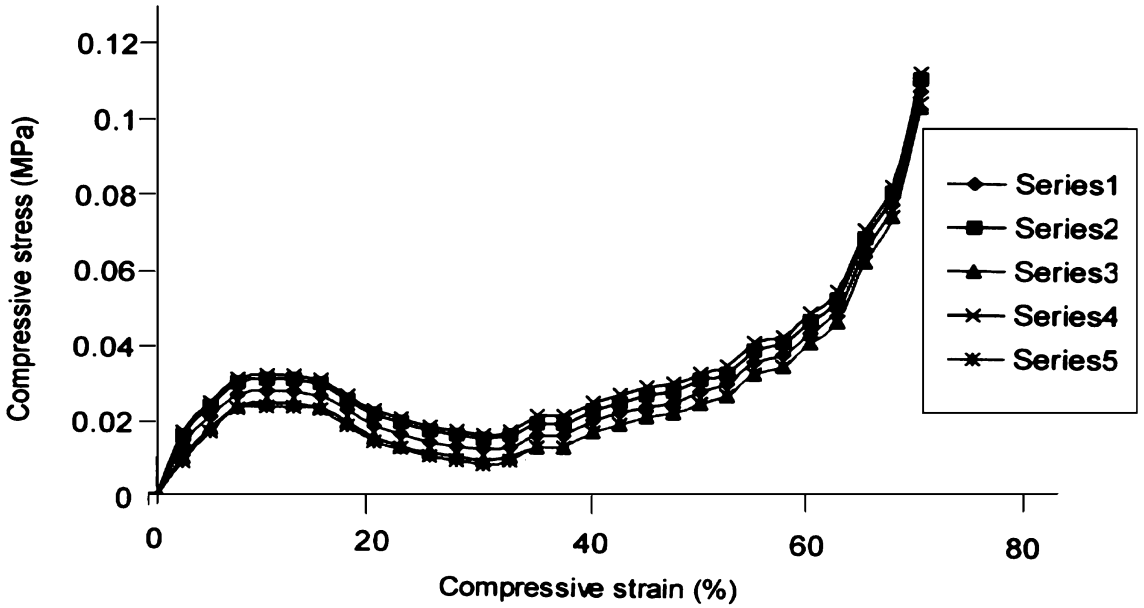

Fig. 7 Compressive stress–strain curves of the sintered porous HAp prepared using PUF 95-600 mold that was taken in five repeated analyses

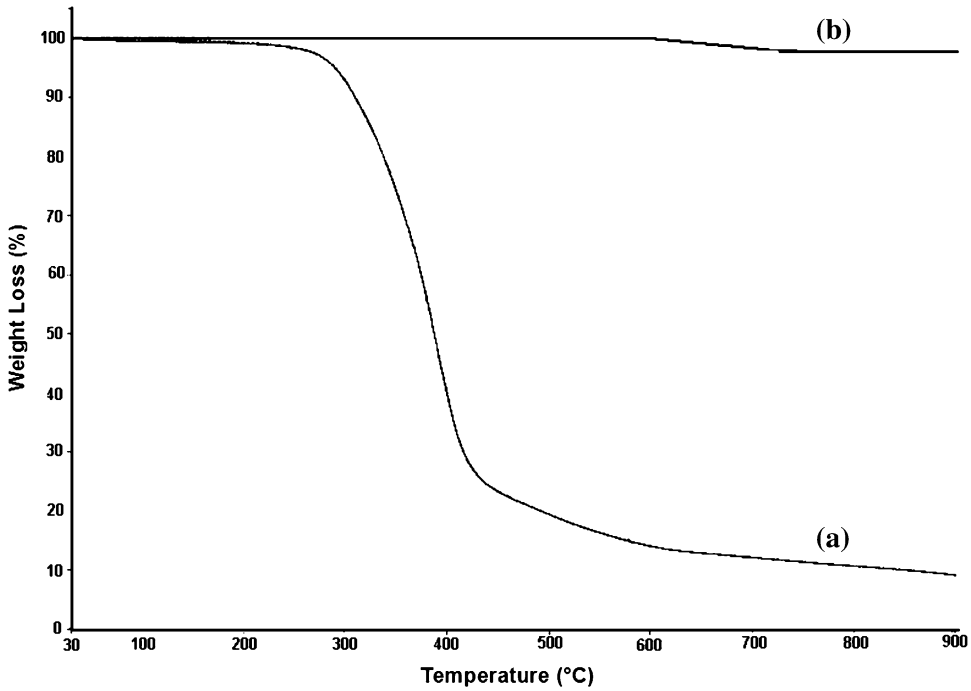

Fig. 8 TGA thermograms of (*a*) PUF and (*b*) porous HAp prepared using PUF 95-600 mold

Figure 6b–d illustrate the shortcomings inherent in the other samples. One of the shortcomings is their susceptibility to structural collapse due to strut failure. Furthermore, although PUFs (PUF 98-1000) with large pore sizes could evenly absorb the CPC slurry, this advantage was negated by their low compressive strength. In contrast, both PUF 60-600 and PUF 25-300 (which contained smaller pores) were more susceptible to slurry blockage and were thus less uniformly coated. It is evident from the above observations that PUF 95-600 with a cell size of 600 μm and a porosity value of more than 95 % was most suitable for use as the mold for porous HAp production.

Figure 7 shows the compressive stress–strain curves of sintered porous HAp prepared using PUF 95-600 mold, which was taken in five repeated analyses on a model sample. The data reveals that sintered porous HAp has lower compressive stress (0.47 ± 0.056 MPa) and strain at 50 % (0.03 ± 0.0036 MPa) when compared to human

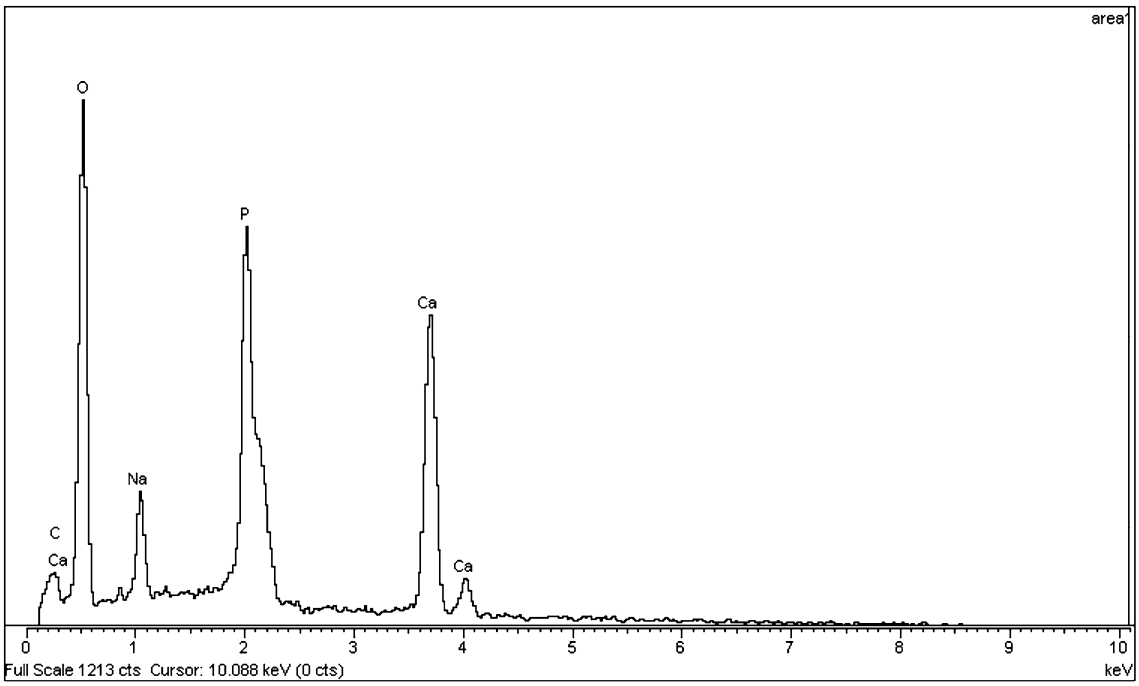

Fig. 9 EDX spectrum of porous HAps prepared using PUF 95-600 mold

bone. Basically, porous hydroxyapatite for bone replacement should possess a compressive strength range of between 2 and 12 MPa [7, 14]. This finding is consistent with recently reported values [7, 9], which reports similar problems. In this regard, it is recommended that the compressive stress of porous HAp be strengthened via further coated (post-treatments) with a bioactive or biodegradable polymers such as poly(lactic-co-glycolic acid), after sintering [15]. Alternatively, the number of dipping into the CPC slurry can be increased in order to further thicken the struts of porous HAp [7].

TGA analysis was used to ensure that the porous HAp was free from PUFs residue. Figure 8 shows the TGA curve for both the PUF and porous HAp samples. It was observed that PUF experienced a weight loss of 93 % above 200 °C which is attributed primarily to polymer degradation. In contrast, the porous HAp sample remained stable up to 700 °C which indicates that the HAp sample was free of PUF residue. This finding is in agreement with that of Miao et al. [7], who noted the same outcome in their research. Nevertheless, HAp exhibited a weight loss of 5 % that might be attributed to the phase transitions in amorphous calcium phosphate from non-stoichiometric to stoichiometric apatites after firing, exceeding temperature of 700 °C [16].

The composition of porous HAp was analyzed by EDX (Fig. 9). It revealed that porous HAp contained 45.69 % oxygen, 3.94 % sodium, 14.09 % phosphorus and 36.30 % calcium. The presence of sodium can be attributed to the use of the setting solution for CPC. Since the total elimination of sodium from CPC was not viable, as it could be structurally attached to the CPC, its removal was deemed to be irrelevant. Moreover, sodium is also found in abundance in the human body, including the bone tissue, and as such pose no threat to human health [17].

4 Conclusion

The porous hydroxyapatite was successfully synthesized using PUF 95-600, with a cell size of 600 μm and a porosity value of more than 95 %, as a mold with CPC slurry with a powder to liquid ratio of 1 g to 0.75 mL. It was also free from PUFs residues despite containing elements such as calcium, sodium, oxygen and phosphorous. This porous HAp met the two criteria for an ideal porous implant which include a cell size of more than 100 μm and a high porosity (>50 %). However, compressive strength of the porous HAp (0.47 ± 0.056 MPa) was reasonable compared to recently reported data, but is still far compared to that of human bone (2–12 MPa). Therefore, further works are required to carry out for improving the mechanical properties.

Acknowledgments The corresponding author wishes to thank to Universiti Malaysia Sabah and Ministry of Higher Education Malaysia for providing funding on UMS grant scheme SLB0020-TK-2012, fundamental research grant scheme, FRG0403-TK-2/2014 and Transdisciplinary research grant scheme, TRGS/2014/UMS/02/2/1/1.

References

1. R. Murugan, S. Ramakrishna, K.P. Rao, Nanoporous hydroxyl-carbonate apatite scaffold made of natural bone. Mater. Lett. **60**, 2844–2847 (2006)
2. X. Miao, W.K. Lim, X. Huang, Y. Chen, Preparation and characterization of interpenetrating phased TCP/HA/PLGA composites. Mater. Lett. **59**, 4000–4005 (2005)
3. M. Mastrogiacomo, S. Scaglione, R. Martinetti, L. Dolcini, F. Beltrame, R. Cancedda, R. Quarto, Role of scaffold internal structure on in vivo bone formation in macroporous calcium phosphate bioceramics. Biomaterials **27**, 3230–3237 (2006)
4. O. Gauthier, J.-M. Bouler, E. Aguado, P. Pilet, G. Daculsi, Macroporous biphasic calcium phosphate ceramics: influence of macroporous diameter and macroporosity percentage on bone ingrowth. Biomaterials **19**, 133–139 (1998)
5. S. Madhavi, C. Ferraris, T.J. White, Synthesis and crystallization of macroporous hydroxyapatite. J. Solid State Chem. **178**, 2838–2845 (2005)
6. G.R. McQuire, D. Green, D. Walsh, S. Hall, J. Chane-Ching, R.O.C. Oreffo, S. Mann, Fabrication of hydroxyapatite sponges by dextran sulphate/amino acid templating. Biomaterials **26**, 6652–6656 (2005)
7. X. Miao, Y. Hu, J. Liu, A.P. Wong, Porous calcium phosphate ceramics prepared by coating polyurethane foams with calcium phosphate cements. Mater. Lett. **58**, 397–402 (2004)
8. P.W. Brown, B. Constantz, *Hydroyapatite and related materials* (CRC Press, Boca Raton, 1994)
9. D. Klempner, K.C. Frisch, *Handbook of polymeric foams and foam technology* (Oxford University Press, New York, 2001)
10. C.S. Sipaut, N. Ahmad, R. Adnan, I.A. Rahman, M.N.M. Ibrahim, Effects of starting material and reaction temperature on the morphology and physical properties of polyurethane foams. Cell. Polym. **29**, 1–25 (2010)
11. D. Guo, K. Xu, K. Han, Influence of cooling modes on purity of solid-state synthesized tetracalcium phosphate. Mater. Sci. Eng., B **116**, 175–181 (2005)
12. G.L.A. Sims, C. Khunniteekool, Cell. Polym. **13**, 137–146 (1994)
13. P.X. Ma, J. Elisseef, *Scaffolding in tissue engineering* (CRC, Taylor & Francis Group, New York, 2005)
14. K. Ishikawa, K. Asaoka, Estimation of ideal mechanical strength and critical porosity of calcium phosphate cement. J. Biomed. Mater. Res. **29**, 1537–1543 (1995)
15. X. Miao, L.-P. Tan, L.-S. Tan, X. Huang, Porous calcium phosphate ceramics modified with PLGA-bioactive glass. Mater. Sci. Eng., C **27**, 274–279 (2007)
16. M. Maciejewski, T.J. Brunner, S.F. Loher, W.J. Stark, A. Baiker, Phase transitions in amorphous calcium phosphates with different Ca/P ratios. Thermochim. Acta **468**, 75–80 (2008)
17. W.L. Suchanek, P. Shuk, K. Byrappa, R.E. Riman, K.S. TenHuisen, V.F. Janas, Mechanochemical-hydrothermal synthesis of carbonated apatite powders at room temperature. Biomaterial **23**, 699–710 (2002)